Conveyor-belt clock synchronization

Vittorio Giovannetti,[1,*] Seth Lloyd,[1,2] Lorenzo Maccone,[1,†] Jeffrey H. Shapiro,[1] and Franco N. C. Wong[1]
[1]*Research Laboratory of Electronics, Massachusetts Institute of Technology, 77 Massachusetts Ave., Cambridge, Massachusetts 02139, USA*
[2]*Department of Mechanical Engineering, Massachusetts Institute of Technology, 77 Massachusetts Ave., Cambridge, Massachusetts 02139, USA*
(Received 26 May 2004; published 12 October 2004)

A protocol for synchronizing distant clocks is proposed that does not rely on the arrival times of the signals which are exchanged, and an optical implementation based on coherent-state pulses is described. This protocol is not limited by any dispersion that may be present in the propagation medium through which the light signals are exchanged. Possible improvements deriving from the use of quantum-mechanical effects are also addressed.

DOI: 10.1103/PhysRevA.70.043808 PACS number(s): 42.50.−p, 03.65.Ta, 06.30.Ft, 89.70.+c

The synchronization of distant clocks is of considerable importance for communications, multiprocessor computations, astronomy, geology, the global positioning system (GPS), etc. Existing synchronization protocols fall into two categories: Eddington adiabatic transfer [1] and Einstein clock synchronization [2]. Eddington's method requires that the two parties (say Alice and Bob) exchange a running clock, e.g., Alice sends her clock to Bob, and he compares it with his own. This method does not require time-of-arrival measurements, but it is usually impractical because a complex system (a clock) must be exchanged. It is much easier to implement Einstein's method, in which all that is exchanged is a sequence of signal pulses, e.g., Alice sends a signal pulse to Bob, which he then returns to Alice. By recording the signal's times of departure and arrival, Alice and Bob can synchronize their clocks. A variation of one or the other of these protocols is invariably employed whenever two clocks must be synchronized [3]: either it is necessary to exchange clocks, or there is an explicit dependence on time-of-arrival measurements. Typical examples of Einstein clock synchronization are the "two way" protocols in which Alice and Bob both exchange signals, phase-locked loop techniques, and pseudorandom code correlation measurements such as are used in GPS.

Here we discuss a synchronization protocol that is neither equivalent to Eddington nor to Einstein synchronization, but instead embodies the best features of each. As in Einstein's scheme, it is based on exchanging signals, thus avoiding the technological problems associated with the exchange of complex systems such as clocks ("shocks on clocks") or entangled systems [4]. As in Eddington's scheme, no time-of-arrival measurements are required, thus avoiding the problems associated with such measurements, e.g., those arising from dispersion in the signal's propagation medium. In this paper we will focus on implementations that rely on classical signals, but the method is well suited for intrinsically quantum-mechanical clock synchronization protocols [5].

In Sec. I we introduce the "conveyor belt" protocol and describe its basic features (some useful variations are discussed in Appendix A). A list of possible implementations in different physical contexts is also given. In Sec. II we present an implementation that relies on polarized laser pulses. Under rather general conditions it is shown that this implementation's attainable synchronization accuracy is unaffected by any dispersion which may be present in the propagation medium. In Sec. III we show how quantum-mechanical effects may be used to enhance the protocol's dispersion suppression: employing frequency-entangled pulses affords dispersion cancellation in even more general circumstances than is the case for implementations using classical (laser) light pulses.

I. "TIME INDEPENDENT" CLOCK SYNCHRONIZATION

In this section we describe in detail the conveyor belt synchronization scheme, which was first proposed in Ref. [5]. The two preconditions that must be satisfied are those underlying Einstein's protocol: (a) we need a physical medium that supports signaling between Alice and Bob in which the Alice-to-Bob and Bob-to-Alice transit times T_{ab} and T_{ba} are identical. (b) We require Alice and Bob to have near-perfect, albeit unsynchronized, clocks, viz., their relative drift is negligible over a roundtrip time $2T$, where $T = T_{ab} = T_{ba}$. (In Appendix A we discuss some variations of our scheme which permit some softening of these requirements.)

Our protocol can be explained by means of a simple illustrative scenario. Suppose that there is a conveyor belt connecting Alice and Bob, as shown in Fig. 1, moving at speed ν. Upon initiation of the protocol, and continuing until its completion, Alice pours sand onto the belt at points A and A' according to the following schedule: when her clock reads t^a she deposits sand at rate $st^a/2$ at both A and A'. Bob, for his part, removes sand at rate st^b from point B when his clock reads t^b. Alice completes the protocol by monitoring the amount of sand at point D—which is after point A' on the conveyor belt—as a function of t^a, and waiting for it to stabilize to a constant value Q_D. It is easy to see that Q_D is

*Present address: NEST-INFM & Scuola Normale Superiore, Piazza dei Cavalieri 7, I-56126, Pisa, Italy.
†Present address: QUIT—Quantum Information Theory Group Dipartimento di Fisica "A. Volta," Università di Pavia, via A. Bassi 6, I-27100, Pavia, Italy.

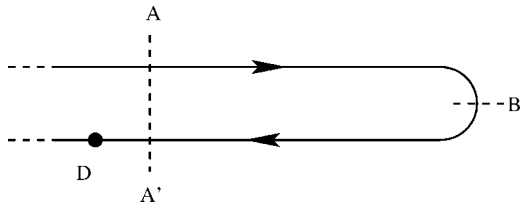

FIG. 1. Representation of the conveyor belt synchronization scheme. Alice pours sand on the conveyor belt at positions A and A', while Bob scoops away sand at the intermediate position B. Measuring the amount of sand at position D—once an initial transient has passed—directly reveals the time difference between their two clocks.

proportional to the time difference between Alice's clock and Bob's clock, as we now demonstrate.

In terms of an external reference clock, showing time t, we may express t^a and t^b—the times shown on the clocks in Alice's and Bob's possession—as follows:

$$t^a = t - t_0^a \text{ and } t^b = t - t_0^b. \tag{1}$$

Here, $t_0^b - t_0^a$ is the offset between Alice's clock and Bob's that the conveyor belt protocol is trying to measure. Once the initial transient is over, i.e., when $t \geqslant \max(2T + t_0^a, t + t_0^b)$, we find that

$$Q_D = \frac{s}{2}(t - 2T - t_0^a) - s(t - T - t_0^b) + \frac{s}{2}(t - t_0^a) \tag{2}$$

$$= s(t_0^b - t_0^a), \tag{3}$$

where the first term on the right-hand side of Eq. (2) is the amount of sand that Alice deposited at point A at time $t - 2T$, the second term is the amount of sand that Bob removed from point B at time $t - T$, and the third term is the amount of sand that Alice added at position A' at time t.

The three main features of this scheme are (1) no time measurements are needed, (2) the only role played by the signal transit time between Alice and Bob is setting the duration of the transient that must be endured before the synchronization measurement can be made, and (3) the synchronization precision only depends on the precision with which sand may be added to, removed from, and measured on the conveyor belt.

That our protocol differs dramatically from Einstein synchronization can be seen from the fact that ours is transit-time independent, i.e., except for its impact on the duration of the conveyor-belt transient, the transit time T—hence the distance between Alice and Bob, $L = \nu T$—plays no role in the protocol. Indeed, neither Alice nor Bob need to know T to run the protocol, nor can they to deduce this transit time by measuring the post-transient amount of sand on the belt at point D. A simple modification of our scheme, however, does permit T to be measured, so that the distance between Alice and Bob may be inferred if ν is known: Alice continues to add sand at rate $st^a/2$ at point A, Bob ceases any action at point B, and Alice removes sand at rate $st^a/2$ from point A'. Once the ensuing transient is over, the amount of sand on the conveyor belt at point D will be

$$Q_D = \frac{s}{2}(t - 2T - t_0^a) - \frac{s}{2}(t - t_0^a) = -sT. \tag{4}$$

If we use microwave signal propagation in lieu of a conveyor belt and the imposition of a positive (negative) frequency shift instead of adding (removing) sand, the ranging protocol we have just described is then the familiar frequency-modulated continuous wave (FMCW) radar [6].

Now, having illustrated the essentials of conveyor belt clock synchronization in terms of the sand-based protocol, let us address more realistic implementations. Alice and Bob may exchange electrical signals, whose voltages are modulated in accord with the conveyor belt idea. Alternatively, they may transmit sound waves (as in sonar applications), modulating their frequencies to achieve clock synchronization via our protocol. The most appealing scenario, however, involves light pulses. In this context Alice and Bob may encode synchronization information on the pulses using the polarization direction (through Faraday rotators), frequency (through acousto-optic modulators), or phase (through electro-optic modulators). An application of this type is analyzed in the next section.

II. DISPERSION-IMMUNE SYNCHRONIZATION

Dispersion-induced pulse spreading and pulse distortion are among the principal performance-limiting factors in schemes that are currently used to synchronize distant clocks [3]. We can exploit our protocol's independence of time-of-arrival measurements to devise synchronization schemes that thwart the ill effects of dispersion. In a previous paper [5] we achieved this goal by means of quantum-mechanical effects. Here, we show that classical pulses can be used to achieve similar dispersion immunity under a wide range of conditions.

The configuration for classical light-pulse clock synchronization via the conveyor belt protocol is shown in Fig. 2. In essence, it is a polarization-based, time-delay interferometer. A linearly polarized (say $\updownarrow$) laser source emits intense light pulses of center frequency ω_0 and bandwidth $\Delta\omega$. Conveyor-belt encoding and decoding is achieved by means of time delays. In particular: at points A and A', Alice delays the 45° ($\nearrow$) polarization with respect to the −45° ($\nwarrow$) polarization by an amount proportional to the time shown on her clock and at point B, Bob delays the −45° polarization with respect to the 45° polarization by an amount proportional to the time shown on his clock, with Bob's proportionality constant being twice Alice's. The net effect of these actions, as seen at the input port to the polarizing beam splitter PBS, is to delay the $\nearrow$ component of the returning light pulse relative to that pulse's $\nwarrow$ component by $\tau_D = \beta(t_0^b - t_0^a)$, where β is Bob's proportionality constant (a dimensionless quantity). Alice now obtains the desired synchronization information by measuring $J_{\leftrightarrow}$, the average photon number in the horizontally-polarized component of the return pulse, by means of the polarizing beam splitter and the integrating photodetector $D_{\leftrightarrow}$. Because no time-of-arrival information is sought in this measurement, dispersion can be neglected if the $\nearrow$ component encounters the same dispersion as its $\nwarrow$ counterpart. As

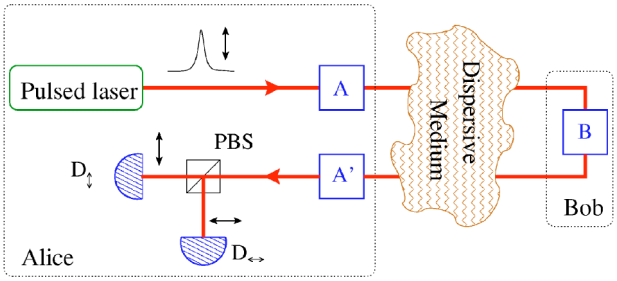

FIG. 2. Proposal for dispersion-immune synchronization. The laser produces intense ↕-polarized pulses that travel from Alice to Bob, where they are reflected back to Alice. At points A and A', Alice delays the 45° polarization with respect to the −45° polarization by an amount proportional to the time shown on her clock. At point B, Bob delays the −45° polarization with respect to the 45° polarization by an amount proportional to the time shown on his clock. These delays are in accord with the conveyor belt protocol, i.e., Bob's proportionality constant is twice Alice's. The polarizing beam splitter PBS separates the incoming beam into its ↕ and ↔ polarization components. These components are directed to integrating detectors $D_{\updownarrow}$ and $D_{\leftrightarrow}$ respectively, which measure the number of photons impinging on them. As discussed in the text, signal multiplexers allow pulses to travel through the dispersive medium in a common polarization state, thus avoiding polarization-dependent propagation effects.

shown below, where we analyze the behavior of the Fig. 2 system, this common-mode dispersion condition can be relaxed in several ways.

Before delving into the mathematics, an initial comment about our theoretical approach is warranted. We will employ quantum photodetection theory in our treatment, despite the fact that semiclassical (shot-noise) theory is quantitatively correct for the Fig. 2 system because it uses coherent-state (classical) light [7]. Our choice in this regard makes it more difficult to connect our work to the literature on laser radar [8], which relies on semiclassical theory and could be used, e.g., to address the performance of time-of-arrival measurements for light-pulse Einstein synchronization. Our reason for choosing to use quantum theory is to enable an easy transition to assessing the additional benefits that accrue from the use of nonclassical light—specifically entangled states—in conveyor belt synchronization. Semiclassical photodetection is unable to treat such systems correctly.

The average photon flux arriving at detector $D_{\leftrightarrow}$ at time t is given by [9]

$$I_{\leftrightarrow}(t) = \langle \Psi | E_{\leftrightarrow}^{(-)}(t) E_{\leftrightarrow}^{(+)}(t) | \Psi \rangle, \tag{5}$$

where $|\Psi\rangle$ is the quantum state of the light emitted by the source and the field operators at the detector are given by

$$E_{\leftrightarrow}^{(+)}(t) = [E_{\leftrightarrow}^{(-)}(t)]^{\dagger} = \int d\omega A_{\leftrightarrow}(\omega) e^{-i\omega t}. \tag{6}$$

The annihilation operator $A_{\leftrightarrow}(\omega)$ destroys a ↔ polarized photon of frequency ω at the location of detector $D_{\leftrightarrow}$. The average photon flux arriving at detector $D_{\updownarrow}$ is obtained in a similar manner. In order to connect the operators $A_{\leftrightarrow}(\omega)$ and $A_{\updownarrow}(\omega)$ with those at the source, we first express the ↕ and ↔

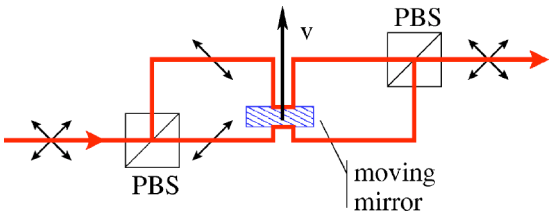

FIG. 3. Model of the time-varying delays introduced by Alice at points A and A' in the Fig. 2 system. The left polarizing beam splitter (PBS) separates the two polarization components so that they impinge on opposing faces of a mirror moving at speed v in the direction shown. The right PBS recombines the polarizations. Bob uses a similar setup at point B in the Fig. 2 system, but his mirror moves at speed $2v$ in the opposite direction from what is shown here. Electro-optic modulators would be used, instead of the moving mirror, in an actual system.

components in terms of their ↗ and ↖ counterparts

$$A_{\leftrightarrow}(\omega) = \frac{1}{\sqrt{2}}[A_{\nearrow}(\omega) - A_{\nwarrow}(\omega)], \tag{7}$$

$$A_{\updownarrow}(\omega) = \frac{1}{\sqrt{2}}[A_{\nearrow}(\omega) + A_{\nwarrow}(\omega)]. \tag{8}$$

The annihilation operators $A_{\nearrow}$ and $A_{\nwarrow}$ may be now linked to the corresponding annihilation operators $a_{\nearrow}$ and $a_{\nwarrow}$ at the source position by accounting for the time-varying delays that Alice and Bob impose in the conveyor belt protocol. Their actions are equivalent to what occurs in the Fig. 3 arrangement, in which the two polarizations impinge on opposite faces of a moving mirror. Electro-optic modulators would be employed in an actual application, but the idealized Fig. 3 setup affords us an easy route to calculating the field evolution from the source to the detector.

Alice has two Fig. 3 setups, one at point A and one at point A'. At time t_0^a she starts moving both of her mirrors with constant speed v, imparting—in the nonrelativistic, $v \ll c$, limit—a Doppler frequency shift $v\omega/c$ $(-v\omega/c)$ to the ↖ (↗) polarization of an incoming frequency-ω field, where c is the phase velocity in the propagation medium at frequency ω. Bob, on the other hand, starts moving his mirror—located at position B—at time t_0^b with constant speed $2v$ in the opposite direction to what Alice employs. Thus, his action leads to a Doppler frequency shift $-2v\omega/c$ $(2v\omega/c)$ on the ↖ (↗) polarization of an incoming frequency-ω field. It follows that the overall annihilation operator transformation that we are after is

$$a_{\nearrow}(\omega) \to A_{\nearrow}(\omega) = a_{\nearrow}(\omega) e^{-i\omega\tau_D + i\omega\tau + i\kappa_{\nearrow}(\omega)}, \tag{9}$$

$$a_{\nwarrow}(\omega) \to A_{\nwarrow}(\omega) = a_{\nwarrow}(\omega) e^{i\omega\tau_D + i\omega\tau + i\kappa_{\nwarrow}(\omega)}, \tag{10}$$

where the term $\tau \equiv 2L/c$ accounts for the distance L separating Alice and Bob, and

$$\tau_D \equiv -4v(t_0^b - t_0^a)/c \tag{11}$$

contains the time shift that is needed to synchronize Alice's clock with Bob's. Note that we have neglected propagation

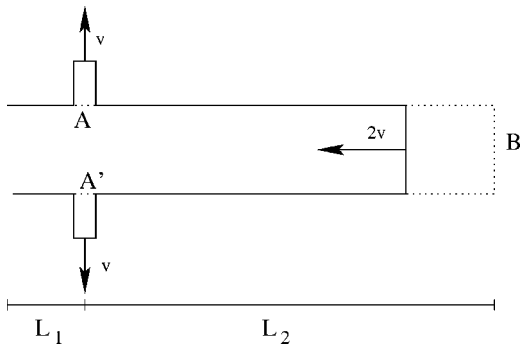

FIG. 4. Explanation of the delay τ_D, from Eq. (11), that is due to the moving mirrors. Prior to the onset of mirror motion, the total optical path length for the $\nearrow$ polarization is $L=2L_1+2L_2$. When the mirrors are moving, by the time the signal reaches point A, the first mirror has increased the path length by $2v(L_1/c-t_0^a)$. This means that the $\nearrow$-polarized signal will incur a propagation delay $(L_1+L_2)/c+2v(L_1/c-t_0^a)/c$ en route to point B. However, during this time interval, Bob's mirror has reduced the path length for the $\nearrow$ polarization by $4v[(L_1+L_2)/c+2v(L_1/c-t_0^a)/c-t_0^b]$. Proceeding in a like manner for the path length increase at A', and summing up all the contributions, we can show that the overall delay τ_D is given by Eq. (11) to first order in v/c.

loss in the roundtrip between Alice and Bob. Because we assume coherent state light in our classical clock synchronization protocol, no loss of generality ensues from this assumption. In essence, any propagation loss in an actual implementation can be accounted for by attenuating the input state used in the analysis below.

The τ_D expression in Eq. (11) is easily derived in the nonrelativistic limit $v \ll c$ by observing that $4v(t_0^b-t_0^a)$ is the path length increase which the interferometer introduces for the $\nwarrow$ polarization relative to the $\nearrow$ polarization (see Fig. 4). In Eqs. (9) and (10) the terms

$$\kappa_{\nearrow}(\omega) \equiv \kappa^t_{\nearrow}(\omega) + \kappa^f_{\nearrow}(\omega), \tag{12}$$

$$\kappa_{\nwarrow}(\omega) \equiv \kappa^t_{\nwarrow}(\omega) + \kappa^f_{\nwarrow}(\omega) \tag{13}$$

represent the dispersive propagation medium encountered by the $\nearrow$ and $\nwarrow$ polarizations; t refers to propagation *to* Bob, while f refers to propagation *from* him. We neglected Doppler frequency shifts in deriving these dispersion terms; see Appendix B for a fully relativistic calculation. Equations (9) and (10) show that our interferometer encodes the time-difference information into both polarization components, whereas for synchronization purposes it would be sufficient to encode such information on just one. (Thus, the scheme adopted here is an instance of the differential conveyor belt protocol described in Appendix A.) However, as will be clarified later, the use of only one polarization component does not provide dispersion immunity.

The initial state of the system is a $\updownarrow$-polarized coherent-state light pulse. It can be described in the frequency domain as a tensor product of monochromatic coherent states of the form

$$|\Psi\rangle \equiv \bigotimes_{\omega} |\alpha(\omega)\rangle_{\updownarrow}|0\rangle_{\leftrightarrow} = \bigotimes_{\omega} |\alpha(\omega)/\sqrt{2}\rangle_{\nearrow}|\alpha(\omega)/\sqrt{2}\rangle_{\nwarrow}, \tag{14}$$

where the ket subscripts refer to polarizations and $|\alpha(\omega)\rangle$ is a coherent state of frequency ω with amplitude function $\alpha(\omega)$ that has center frequency ω_0 and bandwidth $\Delta\omega$, e.g., a Gaussian. Using Eqs. (7)–(10) to express the $\leftrightarrow$-polarized output field in terms of the $\nearrow$-polarized and $\nwarrow$-polarized input fields and then employing Eq. (14) we obtain

$$I_{\leftrightarrow}(t) = \left| \int d\omega \alpha(\omega) \sin\left(\omega\tau_D - \frac{\kappa_{\nearrow}(\omega) - \kappa_{\nwarrow}(\omega)}{2} \right) \times e^{-i\omega(t-\tau)+i[\kappa_{\nearrow}(\omega)+\kappa_{\nwarrow}(\omega)]/2} \right|^2 \tag{15}$$

for the average photon flux at the $D_{\leftrightarrow}$ detector. Dispersion in the propagation medium enters this expression through sum and difference terms, i.e., $\kappa_{\nearrow}(\omega)+\kappa_{\nwarrow}(\omega)$ and $\kappa_{\nearrow}(\omega)-\kappa_{\nwarrow}(\omega)$. The sum term does not contribute to the output of an integrating detector

$$J_{\leftrightarrow} \equiv \int dt I_{\leftrightarrow}(t). \tag{16}$$

To suppress the difference term—and hence achieve dispersion immunity—the two polarization components must undergo the same dispersion in their roundtrip propagation between Alice and Bob, viz.,

$$\kappa_{\nearrow}(\omega) = \kappa_{\nwarrow}(\omega). \tag{17}$$

Under this constraint, the average photon number satisfies

$$J_{\leftrightarrow}(t_0^b - t_0^a) = 2\pi \int d\omega |\alpha(\omega)|^2 \sin^2[4v\omega(t_0^b - t_0^a)/c], \tag{18}$$

where our notation emphasizes the fact that the average photon number depends on the offset between Alice's clock and Bob's. As shown in Fig. 5, the average photon number consists of an envelope of duration $\sim v\Delta\omega/c$ that is modulated by fringes of frequency $8v\omega_0/c$, which result from interference between the $\nearrow$ and $\nwarrow$ return pulses at the polarizing beam splitter. The mean value of this average photon number fringe pattern is $J/2$, where

$$J \equiv \int dt \left| \int d\omega \alpha(\omega) e^{-i\omega t} \right|^2 = 2\pi \int d\omega |\alpha(\omega)|^2 \tag{19}$$

is the average photon number of the input state (14). (Remember that propagation loss is ignored in our treatment.) The extent of the fringe pattern is set by the clock offset $|t_0^b-t_0^a|$ beyond which the $\nearrow$ and $\nwarrow$ return pulses do not overlap at the polarizing beam splitter, so that no interference occurs. When $t_0^b-t_0^a=0$, the average photon number $J_{\leftrightarrow}(t_0^b-t_0^a)$ vanishes, because the $\nearrow$ and $\nwarrow$ return pulses then arrive in synchrony and in phase, forming a $\updownarrow$-polarized field at the polarizing beam splitter. If we include propagation loss, then the occurrence of a perfect $J_{\leftrightarrow}(0)$ null requires that the $\nearrow$ and $\nwarrow$ pulses encounter the same loss in their roundtrip travel between Alice and Bob. Such will be the case if (a) we model loss by assigning imaginary components to the dispersions $\kappa_{\nearrow}(\omega)$ and $\kappa_{\nwarrow}(\omega)$ and (b) we require that Eq. (17) be

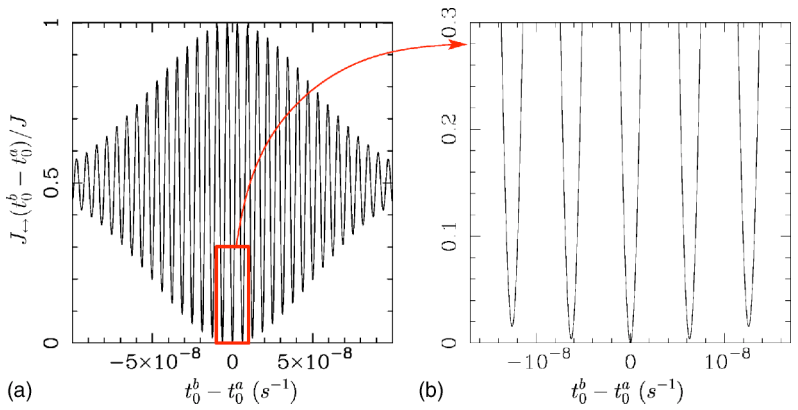

FIG. 5. (a) Plot of $J_{\leftrightarrow}(t_0^b - t_0^a)$ versus $t_0^b - t_0^a$ from Eq. (18) for Gaussian pulses. Here the velocity of the phase variation is $8v\omega_0/c = 10^9\ \mathrm{s}^{-1}$ and the bandwidth is $\Delta\omega = 10^{13}\ \mathrm{s}^{-1}$. (b) Magnification of the box in the previous plot: $J_{\leftrightarrow}(t_0^b - t_0^a)$ has null at $t_0^a = t_0^b$.

satisfied for the resulting complex-valued dispersions.

Alice completes the conveyor-belt synchronization protocol by using a sequence of pulses—shifted in time—to locate the null of the $J_{\leftrightarrow}$ interference pattern (see the last paragraph of Sec. II for a more complete description). The accuracy of such a measurement will be $\sim c/v\omega_0\sqrt{\mathrm{SNR}}$, where $c/v\omega_0$ is the fringe width, and SNR is the measurement signal-to-noise ratio that is achieved with this pulse sequence. When $\mathrm{SNR} \gg 1$, this accuracy can become comparable to the period $2\pi/\omega_0$ of the optical carrier without violating our nonrelativistic constraint, i.e., while maintaining $v \ll c$. Note that Alice can double the SNR of her synchronization by also observing the average photon number $J_{\updownarrow}(t_0^b - t_0^a)$ from the $D_{\updownarrow}$ detector. By energy conservation,

$$J_{\updownarrow}(t_0^b - t_0^a) + J_{\leftrightarrow}(t_0^b - t_0^a) = J, \tag{20}$$

so that this additional measurement has a complementary fringe pattern, whose global maximum is located at the offset between Alice's clock and Bob's.

In essence, our scheme embodies the precision of phase-locking schemes such as Ref. [10], while maintaining the ability to directly recover the time difference between Alice's clock and Bob's. Interestingly, because we measure the average photon number, i.e., the constant quantity $J_{\leftrightarrow}(t_0^b - t_0^a)$, our protocol is immune to dispersion provided that condition (17) is satisfied. How can we enforce such a condition in practice? Usually dispersion in an optical system is polarization dependent, so that Eq. (17) cannot be satisfied directly. However, it is possible to transfer the polarization degree of freedom to other degrees of freedom that undergo the same dispersion. For example, if the medium is sufficiently homogeneous in space, then Alice may send her pulses as copolarized, spatially separated beams—which she recombines in an appropriate interferometer after they return from Bob—to achieve the equivalent of Eq. (17). Alternatively, if the medium is sufficiently stable in time, then Alice may send two copolarized, temporally separated pulses that she recombines in a manner akin to the polarization-restoration scheme described in Ref. [11] to achieve the equivalent of Eq. (17).

Multipulse protocol. Alice needs to identify the global minimum—the null—of the $J_{\leftrightarrow}$ fringe pattern in order to complete the conveyor-belt clock synchronization protocol. In order to do so she will send a sequence of pulses, and employ the resulting $\leftrightarrow$ photon number measurements from the $D_{\leftrightarrow}$ detector. For each pulse, she will vary slightly the delays that she imposes at points A and A', adding a distinct constant $\mathcal{T}_k$ to her starting time t_0^a for the kth pulse, viz., she will treat the first pulse as if her clock's initial time were $t_0^a + \mathcal{T}_1$, she will treat the second pulse as if her clock's initial time were $t_0^a + \mathcal{T}_2$, etc., something she can accomplish without knowing t_0^a. Bob, however, will continue to base his delays on the time shown on his clock. From $\leftrightarrow$ photon number measurements made on this pulse sequence, Alice can estimate the fringe pattern $J_{\leftrightarrow}(t_0^b - t_0^a)$, and hence pinpoint the location of the null.

III. QUANTUM DISPERSION CANCELLATION

The use of quantum resources can improve the performance of traditional clock synchronization and positioning protocols [12]. The same is true for conveyor belt synchronization. In particular, the use of frequency-entangled pulses offers greater immunity to dispersion than is obtainable from the classical version of the protocol, as we now will show. Suppose that the input state to the Fig. 2 interferometer is a stream of time-resolved, frequency-entangled $(\omega_1 + \omega_2 = 2\omega_0)$ biphotons from a type-II phase matched parametric downconverter. Instead of measuring the photon number at the output of the $D_{\leftrightarrow}$ detector, we now detect photon coincidences, i.e., near-simultaneous arrivals of photons at the $D_{\leftrightarrow}$ and $D_{\updownarrow}$ detectors. It can then be shown that condition (17) for dispersion-immune classical operation is replaced by the following less stringent condition under which the quantum system is not degraded by dispersion:

$$\kappa_{\nearrow}(\omega_0 + \omega) + \kappa_{\searrow}(\omega_0 - \omega) = \kappa_{\nearrow}(\omega_0 - \omega) + \kappa_{\searrow}(\omega_0 + \omega). \tag{21}$$

Interestingly, Eq. (21) does not require the two polarization components to undergo the same dispersion: this effect results from the quantum frequency-correlations of the two

photons [13–15]. As shown in Ref. [13], Eq. (21) will be satisfied when the odd-order terms in the Taylor-series expansions of $\kappa_{\nearrow}(\omega)$ and $\kappa_{\nwarrow}(\omega)$ about ω_0 are equal. We now present the essentials of the quantum dispersion cancellation derivation.

The clock synchronization signature that we are seeking is embedded in the probability that the $D_{\leftrightarrow}$ and $D_{\updownarrow}$ detectors both register photons within a coincidence interval whose duration T_c greatly exceeds $1/\Delta\omega$, the reciprocal of the downconverter's fluorescence bandwidth, while still being short enough that the probability of two biphotons being present in this time interval is negligible. This probability can be calculated by considering a biphoton initial state of the following form:

$$|\Psi\rangle \equiv \int d\omega \phi(\omega) |\omega_0 + \omega\rangle_{\nearrow} |\omega_0 - \omega\rangle_{\nwarrow}, \tag{22}$$

where $\phi(\omega)$ is the state's spectral function versus detuning $\omega=0$ from frequency degeneracy, i.e., when both component photons are at the center frequency ω_0. The coincidence probability is then given by

$$\Pr(t_0^b - t_0^a) = \int dt \int_{t-T_c/2}^{t+T_c/2} dt' p(t,t'), \tag{23}$$

where

$$p(t,t') \propto \langle \Psi | E_{\leftrightarrow}^{(-)}(t) E_{\updownarrow}^{(-)}(t') E_{\updownarrow}^{(+)}(t') E_{\leftrightarrow}^{(+)}(t) | \Psi \rangle \tag{24}$$

is the joint probability density for detectors $D_{\leftrightarrow}$ and $D_{\updownarrow}$ to register photons at times t and t', respectively. Unlike the classical case considered earlier, in which the clock synchronization signature appeared in a fringe pattern, the coincidence probability $\Pr(t_0^b - t_0^a)$ exhibits a "Mandel dip" (quantum interference) [16] of width $\Delta\omega^{-1}$ whose null location is specified by the offset between Alice's clock and Bob's:

$$P(t_0^b - t_0^a) \propto \int d\omega |\phi(\omega - \omega_0)|^2 \sin^2[4v(\omega - \omega_0)(t_0^b - t_0^a)/c]. \tag{25}$$

Thus, Alice can perform quantum dispersion-cancelling clock synchronization by a time-shifting procedure similar to what we outlined in the last paragraph of Sec. II for the classical case, obtaining an accuracy $\sim 1/\Delta\omega\sqrt{\mathrm{SNR}}$. An analogous quantum dispersion-cancelling synchronization result was reported in Ref. [5], using a different interferometer.

For the same SNR value, the classical synchronization system will outperform the quantum synchronization system when $v/c > \Delta\omega/\omega_0$, a condition that is unlikely to be satisfied for typical ~THz downconverter bandwidths. On the other hand, we may well inquire whether a frequency-ω_0 fringe pattern might be imposed onto the quantum system's Mandel dip, dramatically enhancing its accuracy. From Ref. [14] it appears that certain experimental configurations allow fringes to be retained with use of the biphoton state (22). As the authors of Ref. [14] point out, however, there is no quantum dispersion cancellation in the regime in which the fringes are present, i.e., when the variable delay in their experiment is placed *after* the beam splitter. In fact, it can be shown that this regime does not exploit the quantum correlation which is present in the state (22): the signal from one of the two detectors is used only to "filter out" a single $\updownarrow$ polarized photon from the state (22) which is then sent into the interferometer. This means that the fringes-present regime in Ref. [14] is equivalent to a single-photon interferometer. So, had the authors of Ref. [14] measured the average photon flux resulting from a coherent-state input—instead of the coincidences resulting from a biphoton input—they would have obtained the same fringes.

IV. CONCLUSIONS

We have presented an optical implementation of the "conveyor belt" clock synchronization protocol that uses classical sources and, under rather general conditions, is not disturbed by the presence of a dispersive medium. The advantages of using quantum sources have been discussed and compared with previous results on the same topic [5].

ACKNOWLEDGMENTS

We acknowledge A. V. Sergienko for interesting comments and suggestions on quantum dispersion cancellation. This work has been supported by the ARDA, NRO, NSF, and by ARO under a MURI program.

APPENDIX A

In this appendix we discuss ways to relax some of the requirements, described in Sec. I, for the conveyor belt synchronization protocol.

1. Differential conveyor belt

So far, we have assumed that the Alice-to-Bob and Bob-to-Alice propagation times are identical, viz., $T_{ab}=T_{ba}=T$. This amounts to having Bob located at the midpoint of the conveyor belt in Fig. 1. We can eliminate this constraint by means of a differential version of our protocol. Differential schemes—such as the two-way method for Einstein clock synchronization—are conventionally employed to get rid of asymmetries. The strategy we choose is to introduce a second conveyor belt that proceeds in the opposite direction with respect to the first one (i.e., it runs from A' to A), as shown in Fig. 6. The protocol is carried out as before: Alice and Bob, respectively, add and remove sand at points A, A', and B, but now they do this on both conveyor belts. After the initial transient is over, the amount of sand that Alice measures at the output of the first conveyor belt (point D_1 in Fig. 6) is given by

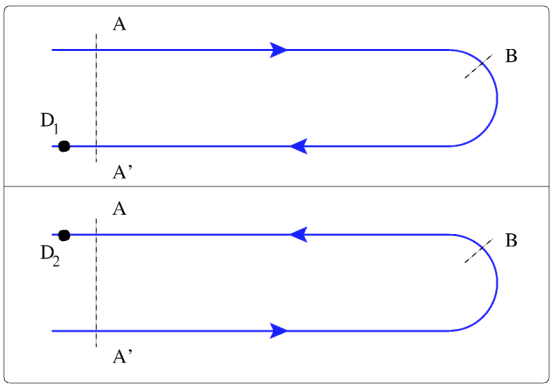

FIG. 6. Differential conveyor belt scheme: Bob is not required to be at the midpoint of the transmission line.

$$Q_{D_1} = \frac{s}{2}(t - T - T' - t_0^a) - s(t - T' - t_0^b) + \frac{s}{2}(t - t_0^a)$$

$$= s(t_0^b - t_0^a) + \frac{s}{2}(T' - T), \tag{A1}$$

where T is the transit time from A to B and T' is the transit time from B to A'. Likewise, the amount of sand that Alice measures, after the initial transient, at point D_2 at the output of the second conveyor belt satisfies

$$Q_{D_2} = \frac{s}{2}(t - T' - T - t_0^a) - s(t - T - t_0^b) + \frac{s}{2}(t - t_0^a)$$

$$= s(t_0^b - t_0^a) + \frac{s}{2}(T' - T). \tag{A2}$$

Clearly,

$$Q_{D_1} + Q_{D_2} = 2s(t_0^b - t_0^a) \tag{A3}$$

provides the desired synchronization information without requiring $T = T'$.

Note that the differential scheme requires that the forward transmission times from A to B and from B to A' equal the backward transmission times from B to A and A' to B, respectively. These equalities can be achieved in optical implementations in which the forward (backward) transmitter and backward (forward) receiver at A (A') are colocated.

2. Imperfect clocks

The requirement that Alice and Bob possess perfect clocks—i.e., that their clocks run at the same rate and do not drift appreciably during a signal roundtrip time—may also be softened. To do so, Alice must monitor the amount of sand on the conveyor belt as a function of time, since it will not be a constant, even after the initial transient has passed. For example, suppose Alice and Bob have drift-free clocks that run at different rates. Insofar as the conveyor belt protocol is concerned, this is equivalent to saying that Alice and Bob have clock's running at the same rate, but that Bob uses proportionality constant s', instead of s, when he removes sand from point B. Equation (2) then becomes

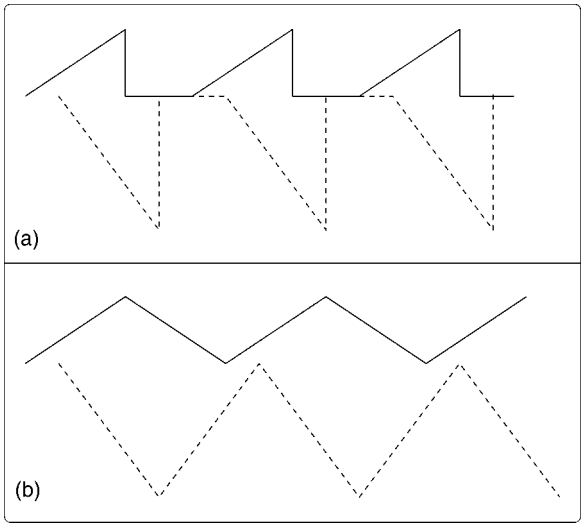

FIG. 7. Two examples of the periodic-ramps protocol. The lines plot the amounts of sand that Alice (solid) and Bob (dashed) must move to (>0) or from (<0) the conveyor belt versus time: (a) Alice and Bob periodically restart the protocol and (b) Alice and Bob periodically reverse their rates.

$$Q_D = \frac{s}{2}(t - 2T - t_0^a) - s'(t - T - t_0^b) + \frac{s}{2}(t - t_0^a)$$

$$= (s - s')(t - T) + s' t_0^b - s t_0^a. \tag{A4}$$

Alice can now use a feedback loop to null out the t-dependent part of Eq. (A4) and thus make her proportionality constant, hence her clock rate, the same as Bob's. A similar procedure will also work if Bob's clock drifts slowly—with respect to the signal roundtrip time—with respect to Alice's.

3. Periodic ramps

The conveyor belt protocol requires Alice to deposit sand at rate $st^a/2$ and Bob to remove sand at rate st^b. With the passage of time, these requirements will soon get out of hand. The essential behavior of the conveyor belt protocol can be retained, however, by periodically restarting the protocol at time intervals that are long compared to both the roundtrip propagation time and the offset between Alice's clock and Bob's. A more convenient alternative might be for Alice and Bob to periodically reverse their rates, as shown in Fig. 7. In fact, this periodic-ramp approach is what is used in FMCW radar [6].

APPENDIX B

In this appendix we derive the relativistic corrections to Eqs. (11)–(13). These corrections only matter if we violate $v/c \ll 1$.

We use Lorentz transformations to go from the source outputs (in the laboratory reference frame), to the fields at the moving mirrors (in the mirrors' reference frames), to the return pulses (back in the laboratory reference frame), as described in Ref. [5]. It is then possible to show that Eqs. (11)–(13) become

$$\tau_D \equiv -\frac{4v/c}{1-(v/c)^2}(t_0^b - t_0^a), \tag{B1}$$

$$\kappa_{\swarrow\nearrow}(\omega) \equiv \kappa^t_{\swarrow\nearrow}(\omega/\chi) + \kappa^f_{\swarrow\nearrow}(\omega\chi), \tag{B2}$$

$$\kappa_{\nwarrow\searrow}(\omega) \equiv \kappa^t_{\nwarrow\searrow}(\omega\chi) + \kappa^f_{\nwarrow\searrow}(\omega/\chi), \tag{B3}$$

where $\chi \equiv (1+v/c)/(1-v/c)$. Moreover, a relativistic correction must also be applied to the delay τ appearing in Eqs. (9) and (10):

$$\tau \equiv \frac{2L}{c}\left(\frac{1+(v/c)^2}{1-(v/c)^2}\right). \tag{B4}$$

[1] A. S. Eddington, *The Mathematical Theory of Relativity*, 2nd ed. (Cambridge University Press, Cambridge, 1924).

[2] A. Einstein, Ann. Phys. (Leipzig) **17**, 891 (1905).

[3] T. Parker, J. Levine, N. Ashby, and D. Wineland (unpublished).

[4] R. Jozsa, D. S. Abrams, J. P. Dowling, and C. P. Williams, Phys. Rev. Lett. **85**, 2010 (2000); R. Jozsa, D. S. Abrams, J. P. Dowling, and C. P. Williams, *ibid.* **87**, 129802 (2001); E. A. Burt, C. R. Ekstrom, and T. B. Swanson, *ibid.* **87**, 129801 (2001); V. Giovannetti, S. Lloyd, L. Maccone, and M. S. Shahriar, Phys. Rev. A **65**, 062319 (2002); U. Yurtsever and J. P. Dowling, *ibid.* **65**, 052317 (2002).

[5] V. Giovannetti, S. Lloyd, L. Maccone, and F. N. C. Wong, Phys. Rev. Lett. **87**, 117902 (2001).

[6] M. I. Skolnik, *Introduction to Radar Systems*, 2nd ed. (McGraw-Hill, New York, 1980), Sec. 3.3.

[7] H. P. Yuen and J. H. Shapiro, IEEE Trans. Inf. Theory **26**, 78 (1980).

[8] G. R. Osche, *Optical Detection Theory for Laser Applications* (Wiley, New York, 2002).

[9] L. Mandel and E. Wolf, *Optical Coherence and Quantum Optics* (Cambridge University Press, Cambridge, 1995).

[10] P. Uhrich, P. Guillemot, P. Aubry, F. Gonzalez, and C. Salomon, IEEE Trans. Ultrason. Ferroelectr. Freq. Control **47**, 1134 (2000).

[11] J. H. Shapiro, New J. Phys. **4**, 47 (2002).

[12] V. Giovannetti, S. Lloyd, and L. Maccone, Nature (London) **412**, 417 (2001); V. Giovannetti, S. Lloyd, and L. Maccone, Phys. Rev. A **65**, 022309 (2002); M. J. Fitch and J. D. Franson, *ibid.* **65**, 053809 (2002)

[13] A. M. Steinberg, P. G. Kwiat, and R. Y. Chiao, Phys. Rev. Lett. **68**, 2421 (1992); A. M. Steinberg, P. G. Kwiat, and R. Y. Chiao, Phys. Rev. A **45**, 6659 (1992).

[14] A. V. Sergienko, M. Atatüre, Z. Walton, G. Jaeger, B. E. A. Saleh, and M. C. Teich, Phys. Rev. A **60**, R2622 (1999); D. Branning, A. L. Migdall, and A. V. Sergienko, *ibid.* **62**, 063808 (2000).

[15] E. Dauler, G. Jaeger, A. Muller, A. L. Migdall, and A. V. Sergienko, J. Res. Natl. Inst. Stand. Technol. **104**, 1 (1999); J. Peřina Jr., A. V. Sergienko, B. M. Jost, B. E. A. Saleh, and M. C. Teich, Phys. Rev. A **59**, 2359 (1999).

[16] C. K. Hong, Z. Y. Ou, and L. Mandel, Phys. Rev. Lett. **59**, 2044 (1987).